International Journal of Biological Macromolecules 184 (2021) 955–966

Contents lists available at ScienceDirect

International Journal of Biological Macromolecules

journal homepage: www.elsevier.com/locate/ijbiomac

Production of functional human fetal hemoglobin in *Nicotiana benthamiana* for development of hemoglobin-based oxygen carriers

Selvaraju Kanagarajan [a], Magnus L.R. Carlsson [a], Sandeep Chakane [b], Karin Kettisen [b], Emanuel Smeds [c], Ranjeet Kumar [d], Niklas Ortenlöf [c], Magnus Gram [e], Bo Åkerström [c], Leif Bülow [b], Li-Hua Zhu [a,*]

[a] Department of Plant Breeding, Swedish University of Agricultural Sciences, Lomma, Sweden
[b] Division of Pure and Applied Biochemistry, Department of Chemistry, Lund University, Lund, Sweden
[c] Division of Infection Medicine, Department of Clinical Sciences in Lund, Lund University, Lund, Sweden
[d] Department of Biology and Biological Engineering, Chalmers University of Technology, Gothenburg, Sweden
[e] Pediatrics, Department of Clinical Sciences Lund, Lund University, Skåne University Hospital, Lund, Sweden

ARTICLE INFO

Keywords:
HBOCs
Fetal hemoglobin
Heme-binding protein
Plant-made pharmaceuticals
Plant molecular farming
Oxygen delivery
Oxygen therapeutics

ABSTRACT

Hemoglobin-based oxygen carriers have long been pursued to meet clinical needs by using native hemoglobin (Hb) from human or animal blood, or recombinantly produced Hb, but the development has been impeded by safety and toxicity issues. Herewith we report the successful production of human fetal hemoglobin (HbF) in *Nicotiana benthamiana* through *Agrobacterium tumefaciens*-mediated transient expression. HbF is a hetero-tetrameric protein composed of two identical α- and two identical γ-subunits, held together by hydrophobic interactions, hydrogen bonds, and salt bridges. In our study, the α- and γ-subunits of HbF were fused in order to stabilize the α-subunits and facilitate balanced expression of α- and γ-subunits in *N. benthamiana*. Efficient extraction and purification methods enabled production of the recombinantly fused endotoxin-free HbF (rfHbF) in high quantity and quality. The transiently expressed rfHbF protein was identified by SDS-PAGE, Western blot and liquid chromatography-tandem mass spectrometry analyses. The purified rfHbF possessed structural and functional properties similar to native HbF, which were confirmed by biophysical, biochemical, and *in vivo* animal studies. The results demonstrate a high potential of plant expression systems in producing Hb products for use as blood substitutes.

1. Introduction

Human hemoglobin (Hb) in the red blood cells (RBCs) of vertebrates has an essential role in oxygen transport. With an aging population, increased number of surgical interventions and a reduced amount of blood donors available, meeting the demand for donated blood has become more challenging [1]. Meanwhile, patient refusal of donated blood for religious, ethical or medical reasons further affects the use [2]. These factors have driven efforts to develop "Hemoglobin-based oxygen carriers" (HBOCs) as a potential resource for emergency clinical treatments of acute anemia, resulting from severe blood loss. HBOCs have potential advantages over human blood, such as universal compatibility, better availability, lack of blood-borne pathogen transmission risks, improved rheological properties and enhanced shelf life [3]. Besides blood transfusion, several other fields of oxygen therapeutics, including oxygenation of organs to be transplanted, have been proposed.

Hb is a heterotetrameric heme-protein consisting of four subunits held together by non-covalent interactions. Each subunit contains a heme group, a porphyrin with an iron ion bound in the center, which is capable of binding and releasing oxygen [4]. In humans, a number of different Hb forms have been described, two major types are adult Hb (HbA) and fetal Hb (HbF). HbA is composed of two α- and two β-subunits ($\alpha_2\beta_2$), while HbF consists of two α- and two γ-subunits ($\alpha_2\gamma_2$). HbF is predominantly produced during the last seven months of fetal development in the uterus, accounting for 50-95% of an infant's total Hb, but is gradually replaced by HbA after birth and constitutes less than 1% of total Hb by the age of two years. Transfusion of HbF appears to be advantageous under certain conditions, such as sickle cell disease and β-thalassemia where the function of HbA is impaired [5,6]. Since HbF has higher oxygen (O_2) affinity than HbA [7,8], and in combination with

* Corresponding author at: Department of Plant Breeding, Swedish University of Agricultural Sciences, Lomma, Sweden.
E-mail address: Li-Hua.Zhu@slu.se (L.-H. Zhu).

https://doi.org/10.1016/j.ijbiomac.2021.06.102
Received 13 March 2021; Received in revised form 11 June 2021; Accepted 13 June 2021
Available online 19 June 2021

an increased protein stability [9], it may suggest that HbF is better suited as an HBOC compared to HbA [10]. Furthermore, severely sick preterm infants and extremely low body weight premature infants require blood transfusion to replace blood loss during intensive care and surgery [11–13]. However, transfusion of adult donor blood (containing HbA) to neonates has demonstrated an increased risk of a devastating intestinal disease, necrotizing enterocolitis and immune sensitization [14]. Altogether, this makes HbF may be an interesting future alternative to current RBC transfusions for anemic preterm infants and possibly also in other clinical applications.

Development of HBOCs has been hampered by safety issues and lack of efficient scalable production systems [2]. Extensive efforts have been made to develop HBOCs either using Hbs purified from animal or human RBC, or by designing recombinantly produced Hbs with improved O_2 binding kinetics, reduced nitric oxide (NO) binding, reduced renal toxicity, and other desirable properties; but unfortunately, the progress has been slow [2,7]. Furthermore, the efforts to develop HBOCs through recombinant expression techniques in microbial systems have encountered some additional challenges [15]. This includes inclusion body formation [16], instability of the alpha subunit [17], insufficient capacity to supply heme, and several strategies have been proposed to overcome these obstacles [15]. Heme is a non-covalently bound prosthetic group of Hb, and heme-binding to globin subunits is crucial to yield functionally active Hb [18]. Hb lacking heme (apo-Hb) is unstable and degrades quickly [19]. Addition of heme, or heme precursor, δ-aminolevulinic acid to the medium is thus needed for producing functional Hb in the bacterial system [19,20], this is however cost ineffective. Furthermore, microbial production constitutes a risk of introducing endotoxins to the HBOC-treated patients [21,22]. The presence of endotoxins in the bloodstream may be toxic and can lead to systemic inflammation, septic shock, organ failure and death [23].

Compared with microbial production systems, the production of Hbs in plants offers some significant advantages [24]. Plants are capable of synthesizing heme [25]. This capacity would greatly facilitate production of recombinant Hb. Also, plant expression system has eukaryotic post-translational modification, such as cleavage of N-terminal methionine, which is essential for proteins' functional activity and stability [26]. Moreover, production of therapeutic proteins in plants is regarded as safe due to the absence of human pathogens and no risk of introducing endotoxins. There are in principle two approaches to express proteins in plants, namely stable and transient gene expression. Stable expression approach is time consuming as it requires production of transgenic plants first, and the expression level is often low [27,28]. Recently, agrospray-based transient expression using plant viral vectors has been developed for efficient production of heterologous proteins [29–31]. This approach has been demonstrated to produce high-level expression of pharmaceutical proteins in *Nicotiana benthamiana*, which has been considered as a robust, low cost, sustainable and scalable protein factory [32,33] and several of the plant-produced proteins are currently undergoing clinical trials [34].

One major challenge of heterologous production of the heterotetrameric HbF is that free Hb α-subunits are unstable in monomeric form, and only stable in dimeric or tetrameric forms of Hb [35]. Fusion of α- and γ-subunits of HbF (fHbF) has been shown to stabilize the α-subunits that are dependent on a cofactor during and after folding without need of expressing additional chaperones. Furthermore, this ensures an equal level of expression of the α- and γ-subunits [36]. In this study, we fused the α- and γ-subunits to produce a recombinant fused HbF (rfHbF) and transiently expressed it in *N. benthamiana* using a viral vector delivered by *Agrobacterium*. The purified protein was shown to be stable and displayed functional properties similar to native HbF, thus enabling further development towards a possible use as an HBOC.

2. Materials and methods

2.1. Agrobacterium strain

Agrobacterium tumefaciens strain GV3101 was used to deliver the viral vectors into the plant cells in this study.

2.2. Plant material

N. benthamiana plants were grown in a controlled climate growth chamber in biotron at SLU, Lomma, at day and night temperatures of 25 °C and 20 °C, respectively, with 60% relative humidity, 250 μmol m^{-2} s^{-1} photosynthetic photon flux density and 18 h photoperiod throughout the study.

2.3. Construction of viral vectors

Human *α* (HBA1) and *γ* (HBG2) *Hb* genes according to the sequences (accession numbers: P69905 and P69892) in the Uniprot database were codon optimized for *N. benthamiana* and synthesized by Thermo Fisher Scientific. The *Avr*II and *Xho*I restriction sites were added to facilitate cloning. A Kozak sequence (GCCACC) [37] was added in the 5′-UTR of the α-gene and a 12-amino acid linker (3 Gly-Gly-Ser repeats) was added to fuse the α and γ sequences as described previously [36], with the α in the 5′ end position as well as two stop codons at the end of the fused gene. The recombinant and fused gene is denoted as *rfHbF* hereafter. The synthesized *rfHbF* gene was cloned into a tobacco mosaic virus (TMV) based viral vector, pJL-TRBO [38], resulting in the vector, named pJL-TRBO-rfHbF, as shown in Supplementary Fig. S1. After sequence confirmation, the vector was transformed into *A. tumefaciens,* strain GV3101. Similarly, the pJL3:P19 vector harboring the *P19* gene of tomato bushy stunt virus (TBSV) for suppressing posttranscriptional gene silencing was also transformed into this strain for co-application later on.

2.4. Agrospray

Agrobacterium suspensions of pJL-TRBO-rfHbF and pJL3:P19 were prepared separately, as described previously [38]. For agrospray, the two suspensions were diluted to OD of 0.025 at 600 nm first, and then mixed at a 2:1 ratio in favor of pJL-TRBO-rfHbF. *Agrobacterium* suspension of the empty vector pJL-TRBO was also prepared in the same way as stated above to serve as control. The diluted suspensions, supplemented by surfactant, Silwet L-77 (Vac-In-Stuff; Lehle Seeds, Round Rock, TX, USA) at 0.1% (v/v) were sprayed onto mature leaves of 4−6 weeks old *N. benthamiana* using a hand-held spray.

2.5. Sampling of leaves and protein extraction

Leaf samples from non-sprayed and sprayed plants with the pJL-TRBO-rfHbF and pJL-TRBO vectors were collected at day 9 after the spray and kept at -80 °C for further use. Before protein extraction, the frozen leaves were homogenized to fine powder in liquid nitrogen. Proteins were extracted using 2 v/w extraction buffer consisting of 10 mM sodium phosphate buffer (pH 6.0), supplemented with 10 mM sodium metabisulfite and 0.05% plant protease inhibitor cocktail (P9599, Sigma-Aldrich) at 4 °C. To increase protein production level, a second spray was done after harvesting initially sprayed leaves, altogether *ca.* 30−40 g of leaves (fresh weight) could be harvested per plant.

2.6. Protein purification

The rfHbF protein purification steps included heating in the presence of carbon monoxide (CO), addition of polyvinylpolypyrrolidone (PVPP), dialysis and chromatography purification. For heat treatment, the total soluble protein extract, saturated with CO with addition of 2% (w/v)

PVPP, was kept at 60 °C for 5 min, followed by centrifugation at 12000 rpm for 10 min at 4 °C. Thereafter, the supernatant was decanted, saturated with CO and filtered through a 0.45 μm filter. The filtered protein extracts were dialyzed in 5 mM sodium phosphate buffer (pH 6.0) at 4 °C, overnight, using dialysis flasks (Slide-A-Lyzer, 10 K MWCO, Thermo Scientific). The dialyzed protein samples were filtered through a 0.45 μm filter, saturated with CO and purified using two chromatographic steps as described previously [39]. The first purification step was cation exchange chromatography (CM Sepharose, GE Healthcare), where the column was equilibrated with 10 mM sodium phosphate buffer (pH 6.0) before loading the sample, followed by elution with 70 mM sodium phosphate buffer, pH 7.2. For the second chromatography step, the samples were buffer exchanged to 20 mM Tris-HCl buffer, pH 8.3 and purified using an anion exchange chromatography column (Q-HP, 5 mL, GE Healthcare), pre-equilibrated with the same buffer. The protein samples were eluted with a gradient of 50 mM sodium phosphate buffer containing 100 mM sodium chloride (NaCl), pH 7.2. The purified rfHbF protein was finally concentrated by centrifugation with Vivaspin columns (30 K MWCO, Sartorius) and snap-frozen in liquid nitrogen in the CO-liganded state, and stored at -80 °C until use. Native HbF was purified from whole blood, freshly drawn from umbilical cord blood, as previously described [40].

2.7. Absorbance spectra, ligand binding and oxygen equilibrium curve analysis

Absorbance spectra of rfHbF protein samples in the presence or absence of different ligands were determined using a Cary 60 UV–Vis spectrophotometer (Agilent technologies) in the range of 250–700 nm at room temperature in quartz cuvettes with a 1 cm path length. A carboxy-rfHbF sample was generated by bubbling the sample with CO and then measuring under CO in a sealed cuvette. Oxy-rfHbF was obtained by applying a continuous stream of oxygen to carboxy-rfHbF solution, under strong light. Met-rfHbF was produced by incubation of oxy-rfHbF with an excess of potassium ferricyanide. This solution was then passed through a gel filtration column Sephadex G-25 (5 × 0.5 cm, GE Healthcare) to remove excess ferricyanide. Deoxy-rfHbF was obtained by addition of a few grains of sodium dithionite to the oxidized sample.

2.8. Estimation of rfHbF quantity

The rfHbF protein was quantified using the carboxy-Hb extinction coefficient at 419 nm [41], measured by a Cary 60 UV–Vis spectrophotometer. All assays were carried out with at least three independent biological replicates.

2.9. Analyses of the rfHbF-protein by sodium dodecyl sulfate–polyacrylamide gel electrophoresis (SDS-PAGE) and Western blot

The purity and specificity of rfHbF were determined by SDS-PAGE and Western blot analyses, respectively under reducing conditions. Prior to SDS-PAGE, the protein extracts sampled after different steps of purification as well as native HbF control were heated at 95 °C for 20 min with loading dye, Bolt sample buffer and Bolt reducing agent (Thermo Fisher Scientific). The protein samples were run on Bolt 4-12% Bis/Tris gels (Thermo Fisher Scientific), and stained with Gelcode™ blue safe protein stain or SimplyBlue™ Safe Stain (Thermo Fisher Scientific) according to the manufacturers' instructions, followed by de-staining with Milli-Q water. Western blot was performed according to the manufacturer's instructions (Thermo Fisher Scientific) using an iBlot™ 2 polyvinylidene difluoride (PVDF) Mini Stack and the iBlot™ 2 System, using the default program (Thermo Fisher Scientific). Rabbit polyclonal anti-HbF primary antibody (targeting gamma (γ)-subunit) and goat anti-rabbit IgG secondary antibody conjugated to horseradish peroxidase (HRP) (Thermo Fisher Scientific) diluted 1:2000 in blocking buffer were used for Western blot analysis. The results were visualized using Novex® ECL is a Chemiluminescent Substrate Reagent Kit (Invitrogen) and a ChemiDoc™ MP Imaging System (Bio-Rad).

2.10. Protein identification and molecular weight determination

For protein identification, the purified rfHbF was retrieved by cutting out the band from the SDS-PAGE gel, digested with trypsin, and analyzed by liquid chromatography (LC) (Dionex, Breda, The Netherlands), coupled with quadrupole mass spectrometry (MS/MS). Mass spectrometric data obtained from quadrupole time of flight (Q-TOF) Ultima instrument (Waters, Sollentuna, Sweden) were recorded with charge state of 2 and 3 (SCIBLU Proteomics Resource Centre, Lund University, Lund). For rfHbF protein identification, tandem MS spectra of the tryptic peptides were analyzed using the Mascot Daemon (version 2.3; Matrix Science Ltd., London, UK) database with settings for carbamidomethylation of cysteines fixed and variable oxidation of methionine residues. For molecular weight determination, the protein sample was first further purified by reversed phase HPLC (Agilent 1200 system) using a short C8 column before being analyzed on a Q-TOF mass spectrometer (Bruker Maxis Impact system). The molecular weight of the protein was determined using a deconvolution algorithm (MaxEnt software, Micromass, Manchester, UK) that calculates the weight of the intact non-protonated peptides (Alphalyse A/S, Odense, Denmark). For further identity confirmation and methionine cleavage, the purified rfHbF was transferred from SDS-PAGE to a PVDF membrane by electroblotting. The band corresponding to the rfHbF protein was excised and the sequence of the five N-terminal amino acids of the protein was determined by Edman degradation using a Procise Protein Sequencing System (Applied Biosystems) (Alphalyse A/S, Odense, Denmark).

2.11. Size exclusion chromatography (SEC)

Molecular weight of the rfHbF was determined using SEC. Sample (50 μM, heme equivalent) in 50 mM sodium phosphate buffer, pH 7.4 plus 150 mM NaCl, was loaded onto Superdex® Hiload 16/60, HR column (GE Healthcare) that was pre-equilibrated with the same buffer. The column was connected to an ÄKTA Explorer (GE Healthcare, Sweden), and elution of the sample was monitored at 419 and 280 nm. The molecular weight of the rfHbF was calculated using a calibration curve of the known molecular weight markers.

2.12. Circular dichroism (CD) spectroscopy

CD measurements of rfHbF and native HbF were carried out with a Chirascan spectropolarimeter (Applied Photophysics, Leatherhead, UK). Far-UV (190–260 nm) CD measurements of oxy-rfHbF (concentration of 5.0 μM heme) were performed in 1 mm quartz cuvettes in 100 mM sodium phosphate buffer, pH 7.4 at 4 °C. Data was collected using a bandwidth of 1 nm, a step size of 1 nm and a time per point of 0.5 s. The instrument was flushed with nitrogen at a flow rate of 5 L/min. Spectra were accumulated five times and the values were corrected for buffer contributions. Data was analyzed using Spectra Manager II software (Jasco, Easton, MD, USA). The samples were stored at 4 ± 1 °C prior to far-UV or CD analysis. Thermal stability experiments were monitored from 20 to 90 °C using CD spectroscopy with the samples incubated at each temperature for 5 min before the CD spectra were collected. Melting temperature values were estimated using sigmoidal fits of thermal denaturation curves at 222 nm performed using the OriginLab (version 2018b) Boltzmann function.

2.13. Dynamic light scattering (DLS)

The purified protein was also analyzed by DLS in a Zetasizer APS instrument (Malvern Panalytical). The rfHbF sample was diluted to 0.3 mg/mL in 10 mM phosphate buffered saline (PBS), pH 7.4 and measured at 20 °C with six replicates.

2.14. Oxygen binding assay

Oxygen equilibrium curves of rfHbF and native HbF (concentration of 94 μM heme equivalent) were recorded on an oxygenation-dissociation analyser (BLOODOX-2018 Analyser, Softron Biotechnology, Beijing, China) in 4 mL of BLOODOX-Solution buffer, pH 7.4 (130 mM NaCl (Chinese Medicine Group Chemical Agent, Beijing, China), 30 mM TES (Sigma Aldrich, St Louis, MO, USA) and 5 mM KCl (Chinese Medicine Group Chemical Agent, Beijing, China), at 37 °C, as described previously [42]. P_{50}, a partial pressure of O_2 at which the heme-binding sites in the rfHbF samples are 50% saturated with O_2 was calculated using the formula as mentioned previously [42]. Hill coefficient (n), a measure of co-operativity in O_2 binding was calculated from the Hill plot (log Y/(1-Y) *vs.* log P), where Y was fractional saturation of rfHbF with oxygen and P was the oxygen pressure in mmHg [43].

2.15. Autoxidation kinetics

In order to estimate the autoxidation rate of rfHbF, CO was first removed by bubbling with air under a strong light, which was followed by two G25 PD10 buffer change steps into air equilibrated buffer (100 mM sodium phosphate buffer, 1 mM EDTA, pH 7.4). The oxy- and deoxy-rfHbF spectra (after sodium dithionite addition) were measured to confirm CO removal and the sample was diluted to ~5 μM concentration (heme). Catalase (C40, Sigma-Aldrich) and superoxide dismutase (S9395-15KU, Sigma-Aldrich) were added at ~3 mmol/mol concentration. The samples, in triplicate, were incubated in sealed cuvettes in a water bath at 37 °C, and measurements were taken every 2 h for the first 10 h in a Multiskan GO spectrophotometer (Thermo Fisher Scientific), followed by measurements at approximately, 20–24 h, 51–55 h and 70–74 h the following days, with a similar 2 h interval. Prior to each measurement, the cuvettes were gently inverted twice. The change in absorbance at 576 nm was used to estimate the autoxidation rate, after subtracting from the detected values of the average absorbance at 690–700 nm for each timepoint, to compensate for some apparent variation in overall background. The values were fitted to a single exponential equation with an offset, using excel solver and the nonlinear-GRG solving method.

2.16. Endotoxin assay

The endotoxin content of rfHbF was assessed by a Limulus Amebocyte Lysate (LAL)-kinetic chromogenic assay with method D described in the Section 2.6.14 of the European Pharmacopoeia with the addition of β-glucan blocker to prevent false positives due to β-glucan-like molecules. All measurements were performed by Lonza (Verviers, Belgium). The assay was run along with an endotoxin standard, diluted serially at five standard concentrations (50 EU/mL–0.005 EU/mL), to generate a standard curve to determine the concentration of endotoxin in rfHbF.

2.17. Animal studies

The animal protocols were approved by the Swedish animal ethics committee in Malmö/Lund, Sweden, prior to the study. The purified rfHbF was injected intravenously into female BALB/c mice (Janvier, Le Genest-Saint-Isle, France) in a maximum volume of 0.2 mL to a total amount of 5 mg per mouse. The mice were then euthanized at various time points to collect blood and urine samples. Blood and urine samples were collected at ~5 min, 2, 6 and 24 h after the injection. Weight and body temperature were recorded at 24 h after the rfHbF injection. Surface body temperature was recorded using a non-invasive Mini IR thermometer (Extech 42510A or Hioki FT3701-20) directed to the lower abdominal region of the mice. The mice were euthanized and cardiac puncture used to collect blood in tubes containing sodium citrate. Citrated plasma was generated by centrifugation and frozen at -80 °C until further use.

rfHbF concentrations in plasma and urine samples were measured using a sandwich ELISA assay. Microtiter plates (MaxiSorp, Nunc) were coated with a rabbit polyclonal anti-human HbF antibody ("Bonita", Agrisera AB, Vännäs, Sweden; prepared after immunization with purified human γ-subunit and specific anti-HbF IgG antibodies were affinity purified as described [40]) at 4 μg/mL in PBS and incubated overnight at 4 °C. The plate was washed 4× with wash buffer (PBS-T, Medicago AB, Uppsala, Sweden) and then the wells were blocked with the blocking buffer (1% BSA in PBS-T) overnight at 4 °C. The wells were washed twice with wash buffer followed by addition of either 100 μL of rfHbF standard or diluted plasma or urine samples. The plasma samples and standard rfHbF series were diluted 1:20–1:4000 in blocking buffer containing CD1 murine plasma (Seralab, West Sussex, UK) to equalize the final plasma concentration. The urine samples were diluted 1:50 or 1:250 in blocking buffer. Upon incubation for 2 h at room temperature, the plate was washed 4× with wash buffer. To detect bound rfHbF, 100 μL of sheep anti-human HbF-HRP conjugate (Bethyl Labs, Montgomery, TX, USA), diluted 1:2000 in blocking buffer was added to the plate and incubated for 2 h at room temperature with gentle shaking, protected from light. Upon washing 4× with the wash buffer, the plate was developed with 100 μL TMB single solution (Invitrogen) for about 10 min and absorbance measured at 650 nm. The plasma half-life was calculated using Microsoft Excel software with the Solver add in (Excel 2013). Unpaired *t*-tests were used to verify significant differences between samples from different time-points using GraphPad Prism 9.0.0 (GraphPad Software, La Jolla, CA, USA).

SDS-PAGE and Western blot analyses of the mouse plasma and urine samples were carried out under reducing conditions as described above. Presence of rfHbF in plasma and urine at different time-points was tested by diluting citrated plasma samples 20× in PBS and the urine samples 10× in PBS before loading 4 μL of sample per well.

Urea nitrogen was measured in mouse plasma using the QuantiChrom Urea Assay kit (Cat#DIUR-100, BioAssay Systems, Hayward, CA, USA). Mouse albumin in the urine samples was measured using a mouse albumin ELISA kit (Cat#ab108792, Abcam, Cambridge, UK). Moreover, the urine samples were assayed for creatinine using the QuantiChrom Creatinine Assay kit (Cat#DICT-500, BioAssay Systems, Hayward, CA, USA). Since a small sample size per group was used, nonparametric Kruskal-Wallis analysis of variance for repeated measures (ANOVA) with Dunn's multiple comparison *post hoc* test were chosen to analyze the albumin to creatinine ratio (ACR) and blood urea nitrogen (BUN) data. The data was statistically analyzed using GraphPad Prism 9.0.0 (GraphPad Software, La Jolla, CA, USA) and differences were considered statistically significant if $P < 0.05$.

The presence of rfHbF protein in urine was investigated by reading the absorbance spectra using a UV–Vis spectrophotometer (Multiskan GO Microplate Spectrophotometer, Thermo Scientific). Spectra of carboxy-rfHbF and deoxy-rfHbF were obtained as described previously.

3. Results

3.1. Successful expression of the human HbF protein in plant expression system

In this study, we have expressed rfHbF in *N. benthamiana* leaves through transient expression with the viral pJL-TRBO-rfHbF vector delivered by *Agrobacterium* using the scalable agrospray method. Analysis of protein extracts with SDS-PAGE (Fig. 1a) showed the expression of the rfHbF protein in the leaves sprayed with *Agrobacterium* harboring the target gene, while as expected, no rfHbF bands were detected in the extract of leaves without agrospray or those sprayed with the empty vector. Efficient extraction and purification of target proteins from plant cells are essential for ensuring high recovery of the functional protein. In this study, we achieved high yield and purity of the functional protein through extraction at acidic pH (pH 6), heat treatment, dialysis and two steps of ion-exchange chromatography. The thermo-tolerant nature of

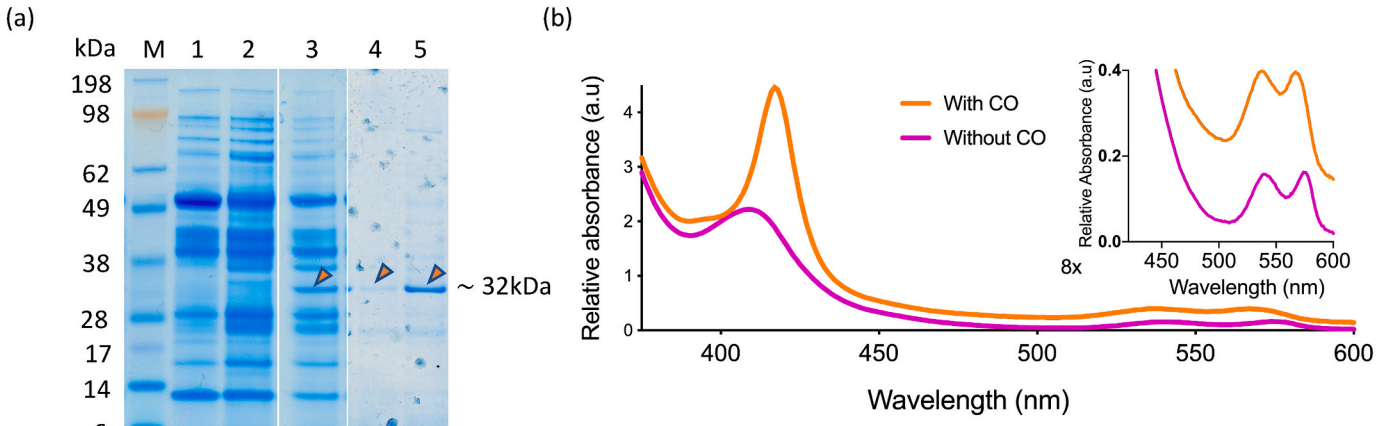

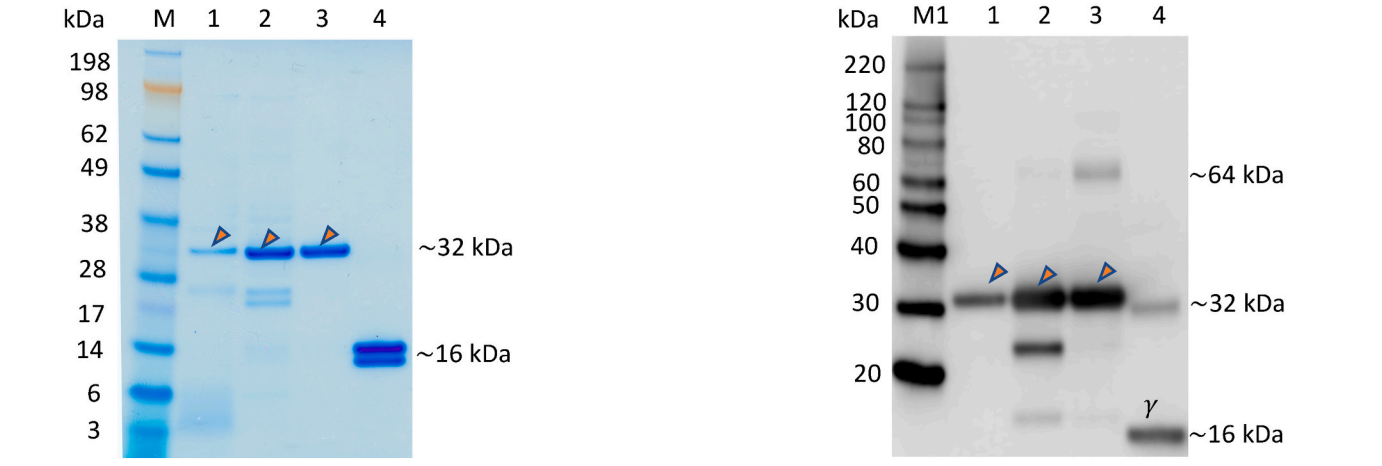

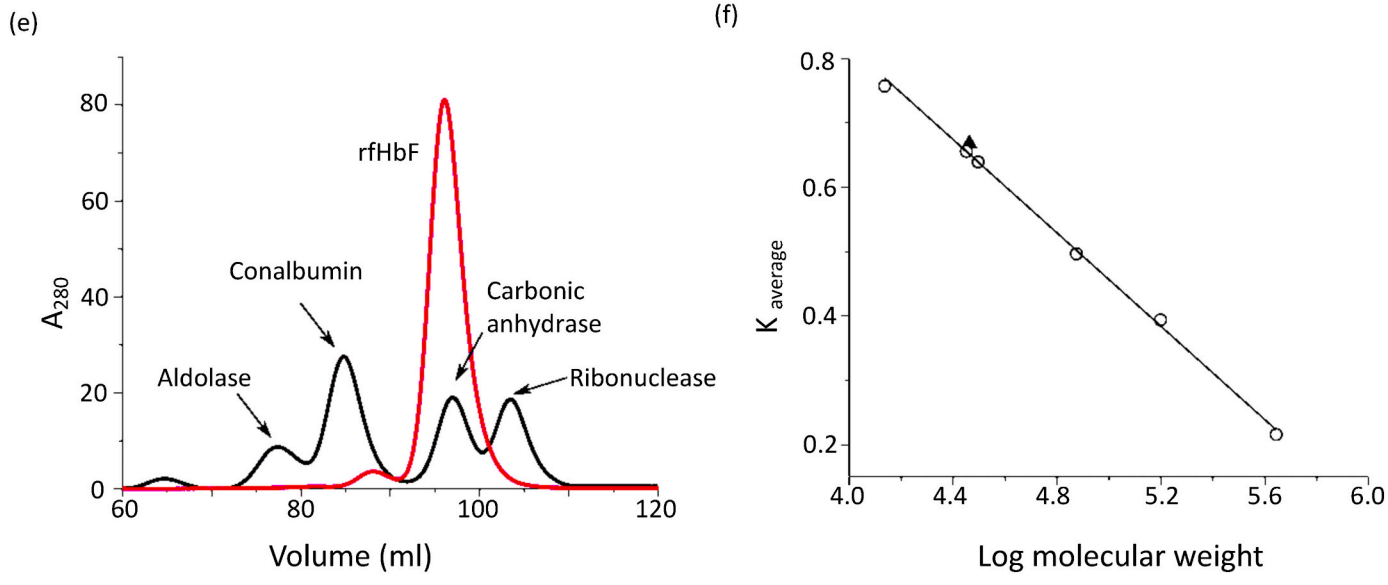

(caption on next page)

Fig. 1. Transient expression, purification, detection and characterization of the rfHbF protein produced in the leaves of *Nicotiana benthamiana*. (a) SDS-PAGE gel showing rfHbF protein from the leaves at day 9 after agrospray. Lane 1, Non-sprayed control; Lane 2, agrospray with empty vector; Lane 3. agrospray with pJL-TRBO-fHbF vector. Image is representative of three independent experiments. Extracts containing 10 μg protein were loaded for each sample. Lane 4, the protein extract non-saturated with carbon monoxide (CO) during heat treatment (60 °C for 10 min); Lane 5, the protein extract saturated with CO during heat treatment (60 °C for 10 min). (b) UV–Vis absorbance spectra of the rfHbF protein extract saturated with CO (orange line) and without CO (purple line) during heating at 60 °C for 10 min with an enlarged insert at 450–600 nm. Data represent the average of three biological replicates. (c) The final purified rfHbF protein of 5 μg on SDS-PAGE gel. (d) The final purified rfHbF protein (5 μg) from Western blot analysis. For (a) and (c) M, SeeBlue™ Plus2 Pre- Stained Protein Standard molecular weight marker with weights (kDa). For (d) M1, MagicMark™ XP Western Protein Standard molecular weight marker with weights (kDa). For (c) and (d), orange arrows indicate the rfHbF bands. Lane 1, sample after heat treatment. Lane 2, sample after cation exchange chromatography. Lane 3, sample after anion exchange chromatography. Lane 4, native HbF. (e) Size exclusion chromatogram showing purified rfHbF. Elution volumes of the calibration standards ferritin (440 kDa), aldolase (158 kDa), conalbumin (75 kDa), carbonic anhydrase (29 kDa) and ribonuclease (13.7 kDa), are indicated. (f) A calibration curve used for determining an apparent molecular weight of rfHbF (closed triangle). (For interpretation of the references to colour in this figure legend, the reader is referred to the web version of this article.)

the carboxy-form of the rfHbF protein helped to preserve the rfHbF structure during heating while removing impurities (Fig. 1b). After purification with cation and anion-exchange chromatography, about 70% of the rfHbF could be recovered with a purity of approximately 95% as estimated by SDS-PAGE (Fig. 1c) and a maximum yield of rfHbF of about 80–100 mg/kg of leaves (fresh weight).

3.2. Protein size verification and size exclusion chromatography (SEC)

The purified rfHbF protein showed a band with the expected molecular weight (~32 kDa of fused α- and γ-subunits of rfHbF) when analyzed by SDS-PAGE (Fig. 1c), and was further confirmed by Western blot analysis (Fig. 1d). No band detected at ~16 kDa (Fig. 1c and d) for rfHbF suggests that the linker that fused the α- and γ-subunits was not disrupted during the protein extraction and purification and was intact in solution. In contrast, the native HbF (Lane 4 in Fig. 1c) migrated as monomeric Hb subunits (~16 kDa), as previously reported under denaturing conditions [44]. The purified rfHbF samples were subjected to SEC in order to probe the homogeneity of the samples and molecular weight of the protein. The peak in the SEC chromatogram corresponds to an apparent molecular weight of 29.3 kDa (Fig. 1e) according to the calibration curve (Fig. 1f).

3.3. Mass spectrometric analysis and N-terminal sequencing of rfHbF

Liquid chromatography-tandem mass spectrometry (LC-MS/MS) was used to confirm the identity of the produced rfHbF protein, covering 43.3% of the amino acid sequence (Fig. 2a). Moreover, ESI-MS was used to measure the molecular weight, which was determined to be 31,906.45 Da (Fig. 2b), closely matching the theoretical molecular weight of rfHbF: 31,906.34 Da, without methionine. N-terminal sequencing confirmed that the rfHbF protein lacked the methionine residue, suggesting efficient removal of the N-terminal methionine in *N. benthamiana* (Supplementary Table S1).

3.4. Biochemical and biophysical characterization

The co-ordination of heme within the Hb subunits is crucial for stabilizing the rfHbF structure and for its O_2 transport capability, however, the oxidation of the ferrous (Fe^{2+}) heme to ferric (Fe^{3+}) heme renders the protein inactive, and may lead to dissociation of heme from the Hb subunits [45]. The detected ultraviolet-visible (UV–Vis) spectra indicated that the rfHbF protein was correctly folded with correct Fe^{2+}, heme cofactor incorporation (Fig. 2c). As shown in the Fig. 2c, the spectra of rfHbF have a single predominant peak in the Soret region, (419 nm for carboxy-rfHbF, 415 nm for oxy-rfHbF, 430 nm for deoxy-rfHbF and 405 nm for met-rfHbF). The longer wavelengths "Q-bands" are also seen in the Fig. 2c at 539 and 569 nm for carboxy-rfHbF, 541 and 576 nm for oxy-rfHbF, as well as the characteristic peaks at 630 nm for the Fe^{3+}, met-rfHbF. The absorbance spectra of rfHbF were very similar to the native HbF as previously reported [10]. The absorbance spectra of rfHbF in the presence and absence of ligands indicate that the rfHbF protein was functional, capable of binding its ligands.

Far-UV circular dichroism (CD) is a powerful analytical tool to determine protein conformation and stability in solution. CD spectra can be used to gain information on the relative proportions of secondary structure elements, α-helical, β-sheet and random coil. To evaluate the secondary structure of the rfHbF protein, we determined its far-UV CD spectra at 190–260 nm (Fig. 2d). Our results showed that the absorbance in the far-UV region was essentially identical for rfHbF and native HbF, indicating that the HbF subunit fusion in rfHbF and the extraction and purification processes did not result in disruptions of the secondary structure (Fig. 2d). A qualitative interpretation of the spectra with double minima around 207 and 222 nm implies that the dominant secondary structure elements in the rfHbF protein are α-helixes, a typical structure of globin proteins contributed by $n \rightarrow \pi^*$ transition for the peptide bond of the α-helix [46]. This is in good agreement with the native HbF [47]. Taken together, these results imply that the subunits of the rfHbF protein produced in *N. benthamiana* are folded identically to the native HbF. To assess the tetrameric state of functional rfHbF, we measured hydrodynamic diameter of rfHbF using DLS and the result showed an average hydrodynamic diameter of 5.3 ± 0.15 nm (standard deviation, n = 6), similar to that of native tetrameric Hb (~5.5 nm) [48]. To determine temperature stability, we also analyzed the CD spectra of oxy-rfHbF and native oxy-HbF at temperatures ranging from 20 °C to 90 °C with 5 °C intervals (Fig. 2e and f). The melting points (T_m) of both native HbF and rfHbF were estimated to be above 60 °C, indicating high thermal stability of both proteins.

3.5. Oxygen equilibrium analysis

We measured the oxygen binding affinity of both rfHbF and native HbF proteins using an oxygenation-dissociation analyser and the results are shown as oxygen equilibrium curves (Fig. 2g). The partial pressure of oxygen at half saturation of the proteins (P_{50}) and Hill coefficient (n) were calculated. The detected P_{50} value (8.94 mmHg) of rfHbF detected was lower than that of native HbF (12.11 mmHg) indicating that rfHbF binds oxygen more tightly, *i.e.*, higher oxygen affinity (Fig. 2g). The calculated Hill coefficients for rfHbF and native HbF were 1.61 and 2.37, respectively, indicating a lower co-operativity of rfHbF compared to the native HbF.

3.6. Autoxidation of rfHbF

The spontaneous oxidation (autoxidation) of Fe^{2+} heme iron to Fe^{3+} in rfHbF was measured in the presence of the antioxidant enzymes, superoxide dismutase (superoxide ion scavenger) and catalase (peroxide scavenger). The detected autoxidation rate of 0.02 ± 0.0014 h^{-1} was comparable to, and slightly lower than, that previously reported for *E. coli* produced rHbF in the presence of catalase (0.03 ± 0.0059 h^{-1}) [49].

3.7. Endotoxin analysis

As we used the gram-negative *Agrobacterium* to deliver the viral vector carrying the target gene into the plant cells, we examined the

(a)

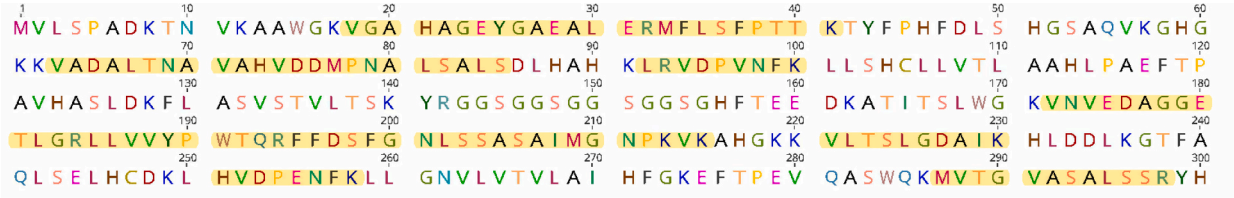

(b)

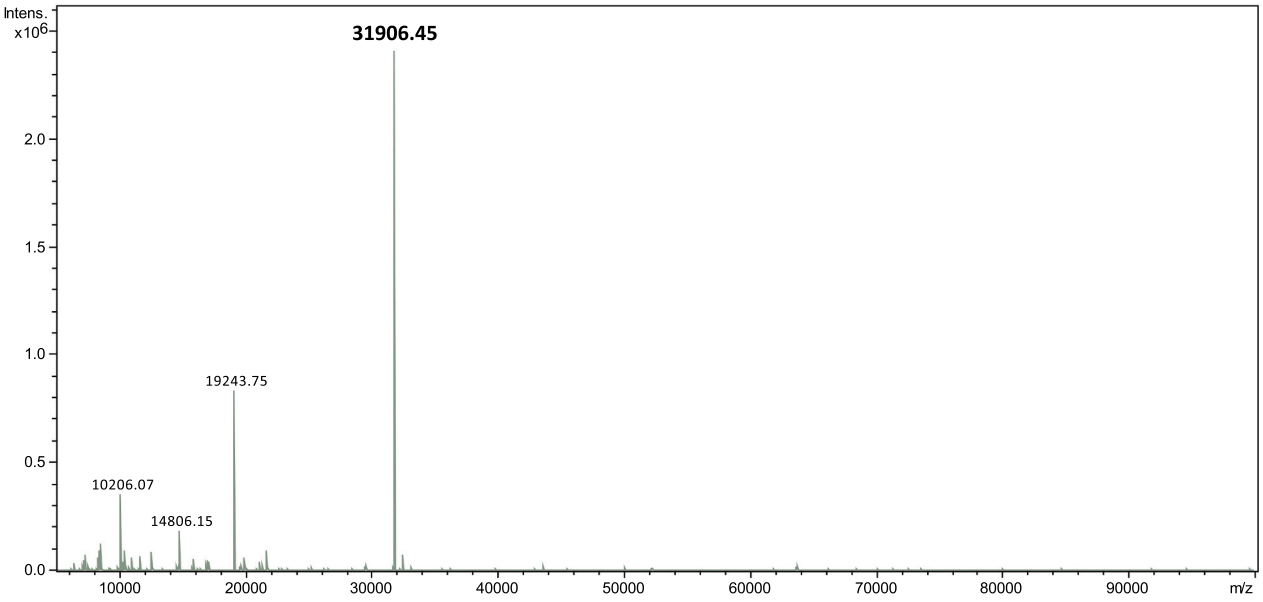

(c)

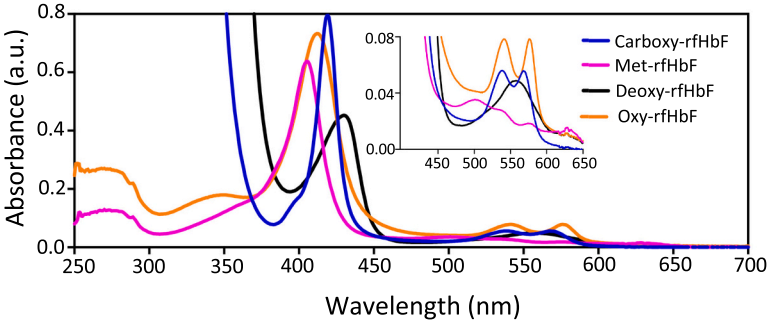

(d)

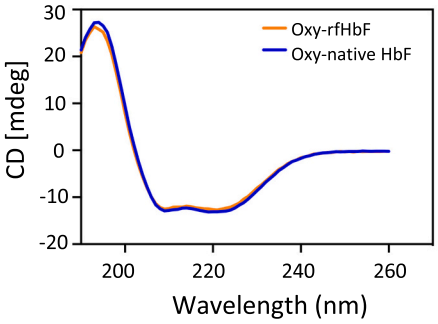

(e)

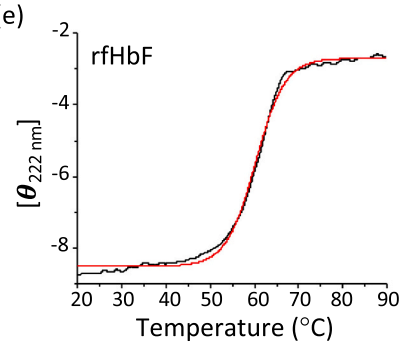

(f)

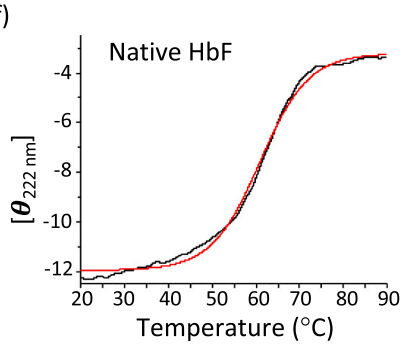

(g)

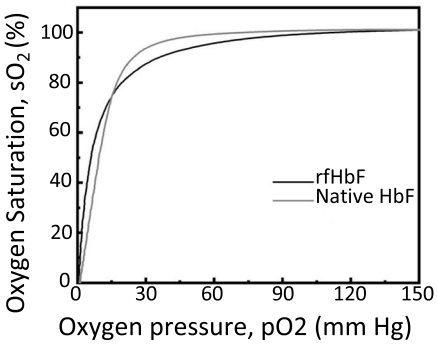

(caption on next page)

Fig. 2. Biophysical and biochemical analyses of purified rfHbF protein extracted from the leaves of *N. benthamiana.* (a) Amino acid sequence and peptide coverage map of rfHbF. Highlighted sequences correspond to peptides detected by liquid chromatography-tandem mass spectrometry (LC-MS/MS) analysis covering 43.3% of the amino acid sequence. (b) Molecular weight (Da) of the purified rfHbF protein was determined using ESI-MS. The molecular weight of rfHbF was 31,906.45 Da, very close to the expected theoretical weight of 31,906.34 Da, indicating correct expression and processing, *i.e.*, the N-terminal methionine was cleaved off. (c) Representative absorbance spectra of rfHbF protein after binding to different ligands, 250–700 nm with an enlarged insert at 450–650 nm. The spectra of rfHbF have a single predominant peak in the Soret peak region at 419 nm for carboxy-rfHbF, 415 nm for oxy-rfHbF, 430 nm for deoxy-rfHbF and 405 nm for metrfHbF, "Q-bands" at 539 and 569 nm for carboxy-rfHbF, 541 and 576 nm for oxy-rfHbF, as well as the characteristic peaks at 630 nm for the met-rfHbF. (d) The secondary structure of rfHbF protein. Overlay of the far-UV (190–260 nm) circular dichroism (CD) spectra of native HbF and plant produced rfHbF. (e) Thermal stability analysis of the oxy-rfHbF by circular dichroism (CD) spectroscopy. (f) Thermal stability analysis of the oxy-native HbF by CD spectroscopy. Boltzmann sigmoidal fit (Red) of CD thermal denaturation curve at 222 nm depicting a melting temperature of 60.3 °C for oxy-rfHbF (Black) and 60.9 °C for oxy-native HbF (Black). The unfolding transitions were monitored after thermal equilibration for 5 min with 5 °C intervals from 20 to 90 °C. (g) Oxygen binding curves of rfHbF and native HbF proteins. The partial pressure of oxygen (pO2) at half saturation of HbF (50% sO_2) was found to be 8.94 mmHg for rfHbF and 12.11 mmHg for native HbF in 130 mM NaCl, 30 mM TES and 5 mM KCl, pH 7.4 at 37 °C. (For interpretation of the references to colour in this figure legend, the reader is referred to the web version of this article.)

endotoxin level along with the purified rfHbF using the Limulus Amebocyte Lysate (LAL) assay. The result showed that the endotoxin level was less than 0.031 units (EU)/mg rfHbF.

3.8. Pharmacokinetic studies of rfHbF in mouse

The pharmacokinetic behavior of rfHbF was evaluated *in vivo* by injecting the purified protein in BALB/c female mice. Urine and plasma samples were collected at ~5 min, 2, 6 and 24 h after the injection. The rfHbF protein could be detected in plasma up to 6 h after the injection, but not at 24 h (Fig. 3a). The calculated half-life of rfHbF in plasma was ~36 min, similar to the previously reported half-life of native HbF [50]. In urine, rfHbF was detected at 2 and 6 h, but not at 5 min or 24 h (Fig. 3b). Albumin to creatinine ratio (ACR) in urine was estimated, to serve as an indicator of kidney functionality. Though ACR was increased after rfHbF injection, it was not significant at any of the time points

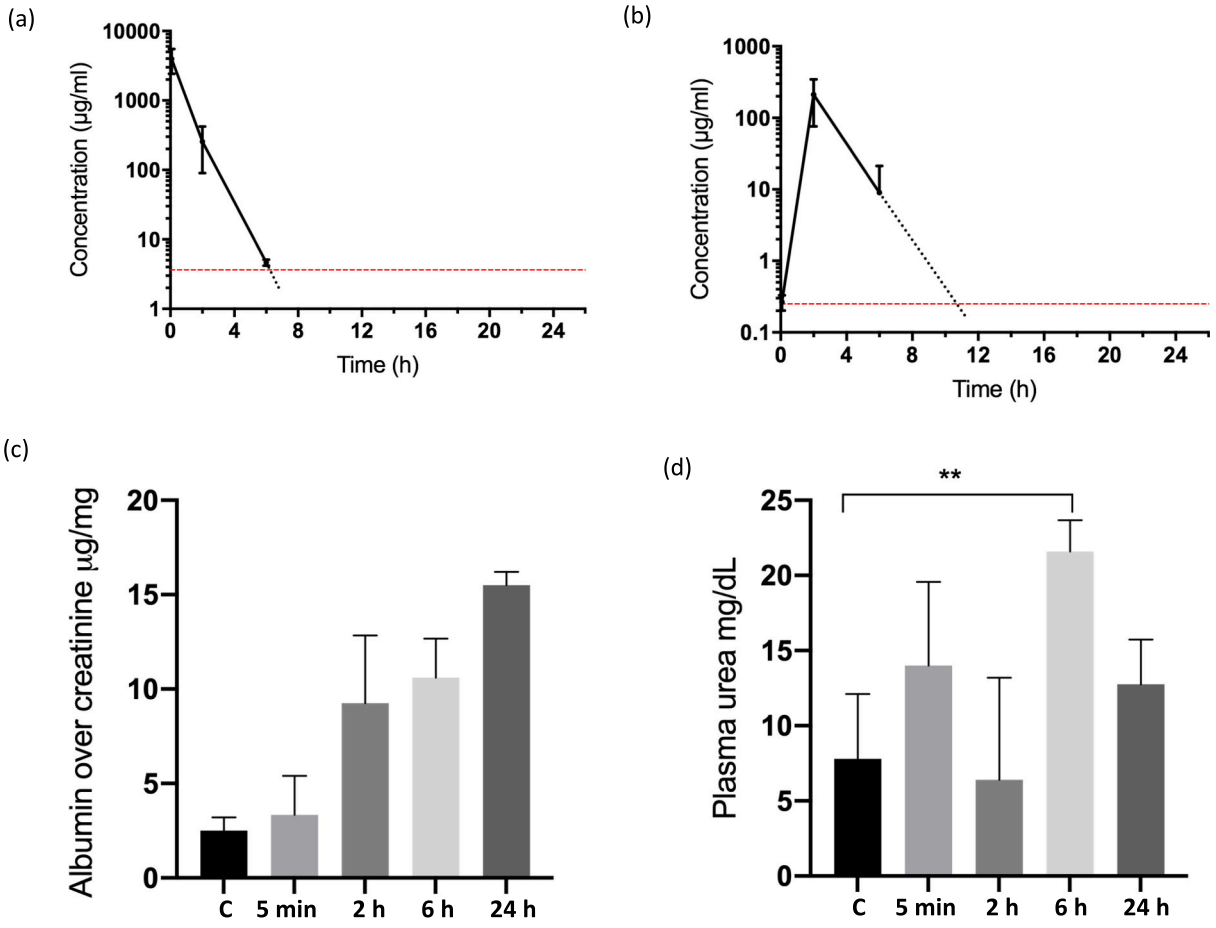

Fig. 3. Pharmacokinetic studies in mice injected with purified rfHbF protein. (a) rfHbF in plasma. (b) rfHbF in urine. For a and b, the analyses were carried out using samples collected at different time-points after the protein injection. The levels of rfHbF were measured using an ELISA assay as described in materials and methods, and are presented as means ± standard deviation (SD). The red dashed line indicates the lower limit of detection in the assay. The black dotted line indicates a hypothetical continued decrease of the rfHbF concentration. (c) Urine albumin to creatinine ratio (ACR) in the mice injected with the protein at 5 min, 2, 6 and 24 h (means ± SD, n = 2–5) (C = Control, non-injected) after the injection. Data was analyzed with nonparametric Kruskal-Wallis test followed by Dunn's multiple parameter post-hoc test using the GraphPad Prism program (GraphPad Software, La Jolla, CA, USA). (d) Blood urea nitrogen (BUN) levels at 5 min, 2, 6 and 24 h (C = Control, non-injected) in plasma samples of the mice injected with rfHbF (means ± SD, n = 2–5). Asterisks above the bar represent statistically significant differences between the treatments at $p \leq 0.01$, analyzed using the same program as stated in (c). (For interpretation of the references to colour in this figure legend, the reader is referred to the web version of this article.)

(Fig. 3c). A significant increase in blood urea nitrogen (BUN) level in the plasma samples was detected at 6 h after the injection, while no significant difference compared to the non-injected control animals were observed at 5 min, 2 and 24 h (Fig. 3d). The weight and body temperature of the rfHbF-exposed mice showed no significant differences compared to the non-exposed mice (Supplementary Table S2).

SDS-PAGE and Western blot analyses showed the presence of rfHbF in plasma at 5 min as well as in the urine sample collected at 2 h, whereas rfHbF was almost non-detectable in plasma at 2 h after the injection (Fig. 4a and b). Since the α- and γ-subunits were fused, the purified rfHbF protein with the molecular weight of ~32 kDa is considered as monomer in this study, equivalent to dimer of native HbF. The Western blot analysis showed the presence of monomeric rfHbF, along with a small quantity of tetrameric and degraded product of rfHbF (Fig. 4b, lane 3) in the urine. The absorbance spectra of rfHbF in the urine samples collected at 2 h after the injection showed a main peak at 410 nm in the Soret region and peaks at 538 nm (β-band) and 576 nm (α-band), suggesting that the protein has preserved its native structure in the urine and is present as a mixture of oxy-rfHbF and met-rfHbF (Fig. 4c).

4. Discussion

The attempts of developing HBOCs through heterologous expression techniques in microbial systems have only been partially successful in the past. One challenge is that Hb production needs to have heme incorporated into the Hb subunits for proper folding and function. However, most microbial production systems produce insufficient heme themselves, which increases the production cost and complicates the production process. Consequently, the expression of Hbs is often accompanied by production of the apo-Hb [51]. Moreover, the bacterial expression systems can cause formation of inclusion bodies, which leads to low production efficiency [52]. For the synthesis of a multisubunit protein, an equimolar ratio between the subunit molecules is necessary. Our initial attempts to produce HbF by co-expression of chimeric α- and γ-subunits in two independent expression vectors with the respective clones of recombinant *Agrobacterium* in *N. benthamiana* was not successful, probably due to unbalanced expression of the α- and γ -subunits. To address the challenges posed by heterologous expression of Hbs in microbial systems, and expressing complex heterodimeric protein in *N. benthamiana*, we have evaluated a plant-based expression system for expressing rfHbF using a viral vector harboring the target gene with

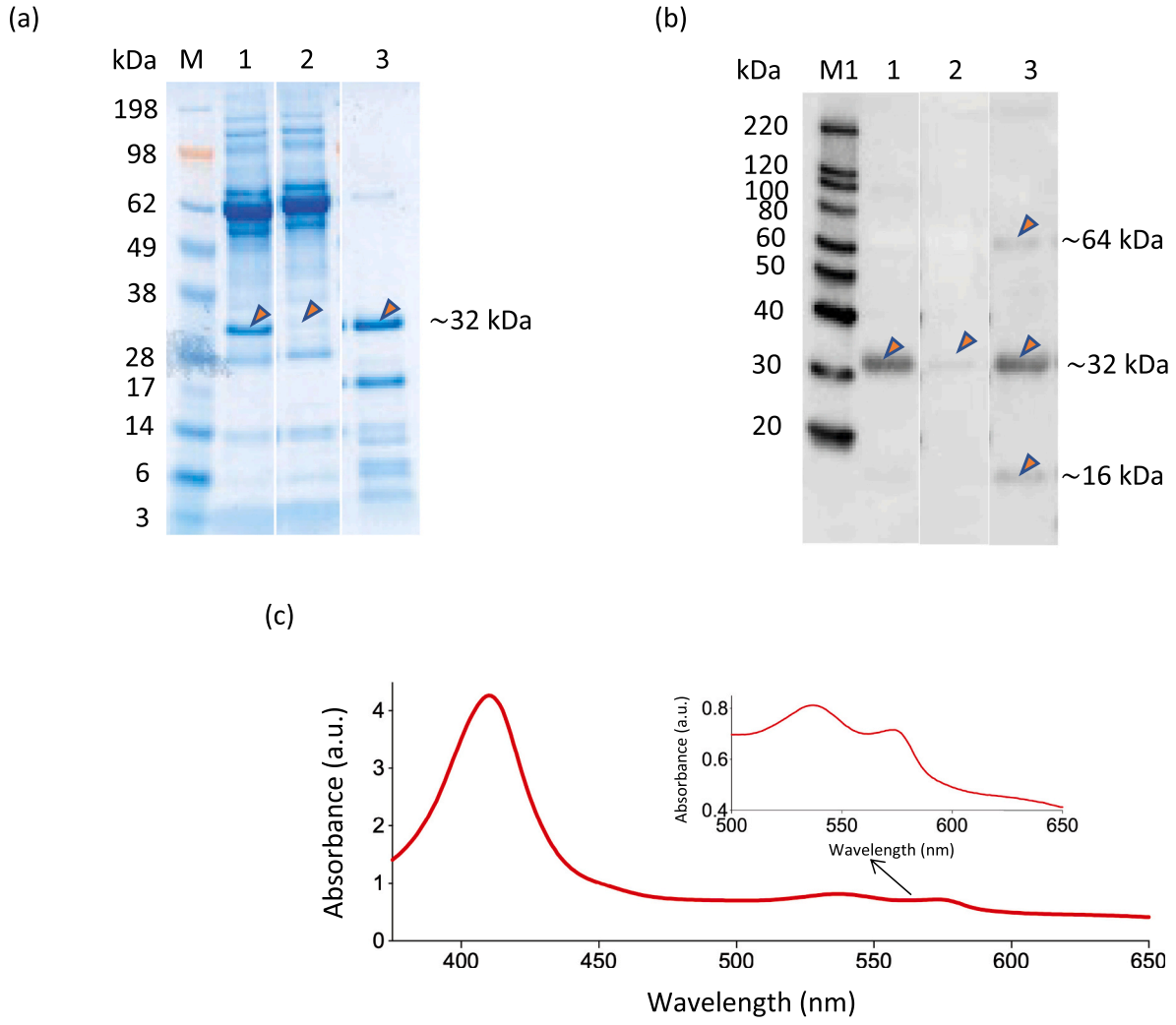

Fig. 4. Detection of rfHbF in plasma and urine of the treated mice. The plasma and urine samples were diluted with phosphate buffered saline (PBS) buffer by 20× and 10×, respectively and analyzed by SDS-PAGE and Western blot. Samples of 4 μl were loaded in each well. (a) SDS-PAGE (b) Western blot. M, SeeBlue™ Plus2 Pre-Stained Protein Standard molecular weight marker with weights (kDa). M1, MagicMark™ XP Western Protein Standard molecular weight marker with molecular weights (kDa). Lanes 1 and 2, the plasma samples collected at 5 min and 2 h after the rfHbF injection, respectively; Lane 3: urine sample collected 2 h after the rfHbF injection. (c) UV–Vis absorbance spectra of mouse urine collected at 2 h after the rfHbF injection. The insert shows the region at 500–625 nm. The spectra of the collected urine sample appeared to show a mixture of met- and oxy-form of rfHbF.

fused α- and γ-subunits, joined by a small peptide linker, a design intended to help stabilize the α-subunit and ensure balanced expression of both subunits. This is, to our knowledge, a novel strategy to produce functional human Hbs in plants.

Heterologous expression of a heterodimeric metallic protein like Hb, requiring specific cofactors, heme, for correct folding adds additional challenges. To produce fully functional rfHbF, proper heme incorporation is essential. It has been shown that the *E. coli* expression system often results in sub-optimal heme incorporation into Hbs due to the limited amount of free heme available in the culture medium, leading to rapid denaturation of the Hb [19]. Our results show that heme seemed to be successfully incorporated into rfHbF, evidenced by correct spectra and limited loss by heat treatment (Hb subunits without heme, apoglobin, often aggregate and degrade quickly at high temperature) [19]. Since rfHbF did not carry any peptide sequence for targeting to a specific compartment, the detection of rfHbF in the agrosprayed leaves in this study indicates that the heme insertion into Hb subunits most likely took place in the cytosol. Studies on subcellular localization of plant Hbs also indicate that they are expressed in the cytosol [53]. As shown in this study (Figs. 1b and 2c), heme incorporation into Hbs in the plant expression system has occurred without need for overexpressing enzymes responsible for heme biosynthesis, possibly indicating the abundant nature of heme in plant cells. However, more studies are required to confirm whether heme availability is a limiting factor for further increased expression levels of Hbs in plants. In plants, heme is synthesized in chloroplasts and mitochondria and delivered to the cytosol [25,54]. It has previously been suggested that the heme-biosynthetic pathway in plants is highly conserved and that the levels of heme are strictly controlled by the retrograde signaling in the chloroplasts to regulate the expression of nuclear genes. Based on the results of this study, we suggest that the overexpression of Hb protein in the cytosol could possibly hijack the heme biosynthetic pathway by interfering with the signal, and thus stimulate overproduction of heme iron in the chloroplast/mitochondria in order to meet the increased cellular demand.

The majority of the host cell proteins (HCPs), including most of the abundant ribulose-1,5-bisphosphate carboxylase oxygenase (RuBisCO) protein [55], could be removed by heat treatment, a convenient and low-cost method [56]. Moreover, many of these host cell proteins including RuBisCO have low solubility at pH 6 [57,58] and their quick removal might have been beneficial for rfHbF stability during the extraction and purification processes. Our results have shown that the heat treatment with extraction buffer at low pH prior to further purification was effective at removing most unwanted compounds, while maintaining the majority of the rfHbF protein. The soluble holo-rfHbF (Hb protein with bound heme) can be quickly separated from the apo-rfHbF by heating, as apo-rfHbF is denatured at high temperature [19]. This has also added the benefit of avoiding interference from active plant enzymes in the later dialysis and column chromatography steps.

Contamination with endotoxins could be a concern since endotoxins are known to be pyrogenic and cause shock reactions in mammals [23]. Our data shows that the expression and purification techniques employed to produce rfHbF is highly effective to minimize and/or remove potentially contaminating endotoxins derived from the *Agrobacterium* inoculums. Agrospray with diluted agrobacterial suspensions (OD_{600}-0.025), protein purification with heating [59], cation- and anion-exchange chromatography, and ultrafiltration were found to reduce the weakly bound low and high molecular weight endotoxins below threshold levels (5 EU per kg of body weight an hour) set by all pharmacopoeias for intravenous applications [60]. The detected endotoxin level (0.031 units (EU)/mg of purified rfHbF) in this studysuggests that the high doses of rfHbF expected to be administered in a possible pharmaceutical use as an HBOC would be acceptable.

The P_{50} value of rfHbF (8.94 mmHg) was slightly lower than that of the non-fused rHbF produced in *E. coli* (9.6 mmHg) [39] and native HbF (12.11 mmHg), suggesting a high oxygen affinity of plant produced rfHbF compared with *E. coli* produced non-fused rHbF and native HbF. The high oxygen affinity of plant produced rfHbF could possibly help prevent premature oxygen off-loading in arterioles preventing vasoconstriction and allowing for downstream O_2 delivery in capillaries [61,62] and may confer a neuroprotective effect in the vulnerable region of the hippocampus [63]. The Hill coefficient (1.61) for rfHbF indicates higher cooperativity of the plant produced rfHbF compared to that of the *E. coli* produced non-fused rHbF (1.20) [39] and a lower cooperativity than native HbF (2.37). The higher affinity and lower cooperativity of rfHbF than native HbF were probably associated with the fusion of α- and γ-subunits in the rfHbF. The higher oxygen affinity property of rfHbF probably would help to deliver oxygen to the most hypoxic tissues [7]. Interestingly, the oxygen therapeutic, Hemospan (MP4) that had gone through early clinical trials exhibited high oxygen affinity ($P_{50} \sim 5$ mmHg) with minimal cooperative oxygen binding (1.2) [61].

Cell free oxygen bound Fe^{2+} Hb is spontaneously oxidized to non-functional Fe^{3+} met-Hb and the subsequent reactions lead to heme damage and eventually heme degradation [64]. Autoxidation of Fe^{2+} Hb is a serious concern for the use of Hb as oxygen therapeutics, as it compromises the function and safety [65]. In this study, it was shown that rfHbF had a slightly decreased rate of autoxidation, as compared to non-fused rHbF produced in *E. coli* [49], suggesting that fusion of α- and γ-subunits does not affect the stability of this protein towards autoxidation. Given the somewhat elevated oxygen affinity observed for rfHbF, a lower autoxidation rate would be in line with the inverse correlation between Hb oxygen affinity and autoxidation rate noted previously [43,64], although other factors such as degree of Hb tetramer formation may also play a role in determining autoxidation rate [66].

The observed half-life (~36 min) of the rfHbF was in agreement with previous studies where it was reported as 0.1 ± 0.1 h in mice infused with native HbF [50]. The detection of rfHbF in the urine sample 2 h after the injection indicates that the rfHbF was rapidly cleared from the blood circulation and filtrated through the glomerulus into the urine. Indeed, an increased level in urinary ACR detected after the injection, supports a transient effect of rfHbF on kidney glomerular permeability. This effect was, however, not significant. This is in agreement with previous study in rats where HbF-injection resulted in a transiently increased glomerular permeability [67]. Furthermore, a significant increase in plasma BUN at 6 h after injection suggests that rfHbF may have a broad effect on kidney glomerular filtration. However, plasma BUN displayed tendencies to return to baseline, *i.e.*, similar levels as the control animals, indicating that the effect of rfHbF is temporary. Altogether, the *in vivo* data indicates that a fusion of the α- and γ-subunits does not seem to be a viable strategy to prolong circulation time. The main reason for fusing the subunits was however to facilitate the protein production rather than extend circulatory half-life. Further improvements of the pharmacokinetic properties are therefore warranted, employing strategies such as further encapsulation or desolvated nanoparticle [4,68] using the described rfHbF as an HBOC platform.

In conclusion, we were able to successfully produce rfHbF in significant quantity in a plant expression system by transient expression using scalable agrospray technique. The rfHbF protein could be efficiently purified to the high degree needed for functional studies *in vitro* and *in vivo*. The purified rfHbF protein was shown to possess structural and functional properties similar to native HbF. The present study has shown the feasibility of producing large amounts of rfHbF in plants, perhaps a first step towards using the plant expression system for production of Hbs for HBOC research and future medical applications.

CRediT authorship contribution statement

Selvaraju Kanagarajan: Conceptualization, Visualization, Methodology, Validation, Formal analysis, Investigation, Data curation, Writing- Original Draft, Review & Editing. **Magnus L. R. Carlsson:** Investigation, Formal Analysis, Writing- Review & Editing. **Sandeep Chakane:** Investigation, Formal Analysis. **Karin Kettisen:**

Investigation, Writing- Review & Editing **Emanuel Smeds:** Investigation, Formal Analysis. **Ranjeet Kumar:** Investigation, Formal Analysis **Niklas Ortenlöf:** Investigation, Formal Analysis. **Magnus Gram:** Methodology, Resources, Writing- Review & Editing. **Bo Åkerström:** Methodology, Resources, Writing- Review & Editing. **Leif Bülow:** Methodology, Resources, Writing- Review & Editing. **Li-Hua Zhu:** Conceptualization, Visualization, Resources, Writing- Review & Editing Project Administration, Supervision, Funding Acquisition.

Declaration of competing interest

The authors declare no conflict of interest with the contents of this article.

Acknowledgements

The authors wish to thank Khuanpiroon Ratanasopa for her help on vector construct preparation, John Lindbo for providing pJL-TRBO and pJL3:p19 vectors, and Lian Zhao and Guoxing You for oxygen binding assay. We also acknowledge the help with the protein analysis from the SCIBLU Proteomics Resource Centre at Lund University and the Wallenberg Stiftelse (KAW). This work was financed mainly by a research grant from the Swedish Foundation for Strategic Research (SSF) to L.B., B.Å., M.G. and L-H.Z. and partially by Trees and Crops for the Future (TC4F), a Strategic Research Area at SLU, supported by the Swedish government, to L-H.Z.

Appendix A. Supplementary data

Supplementary data to this article can be found online at https://doi.org/10.1016/j.ijbiomac.2021.06.102.

References

[1] A. Ali, M.K. Auvinen, J. Rautonen, Blood donors and blood collection: the aging population poses a global challenge for blood services, Transfusion 50 (2010) 584–588.
[2] A.I. Alayash, Blood substitutes: why haven't we been more successful? Trends Biotechnol. 32 (2014) 177–185.
[3] G.G. Silkstone, R.S. Silkstone, M.T. Wilson, M. Simons, L. Bülow, K. Kallberg, K. Ratanasopa, L. Ronda, A. Mozzarelli, B.J. Reeder, Engineering tyrosine electron transfer pathways decreases oxidative toxicity in hemoglobin: implications for blood substitute design, Biochem. J. 473 (2016) 3371–3383.
[4] C. Coll-Satue, S. Bishnoi, J. Chen, L. Hosta-Rigau, Stepping stones to the future of haemoglobin-based blood products: clinical, preclinical and innovative examples, Biomater. Sci. 9 (2021) 1135–1152.
[5] I. Akinsheye, A. Alsultan, N. Solovieff, D. Ngo, C.T. Baldwin, P. Sebastiani, D.H. K. Chui, M.H. Steinberg, Fetal hemoglobin in sickle cell anemia, Blood 118 (2011) 19–27.
[6] T. Dasgupta, M.E. Fabry, D.K. Kaul, Antisickling property of fetal hemoglobin enhances nitric oxide bioavailability and ameliorates organ oxidative stress in transgenic-knockout sickle mice, Am. J. Phys. Regul. Integr. Comp. Phys. 298 (2010) R394–R402.
[7] M. Simons, S. Gretton, Gary G.A. Silkstone, Badri S. Rajagopal, V. Allen-Baume, N. Syrett, T. Shaik, N. Leiva-Eriksson, L. Ronda, A. Mozzarelli, Michael B. Strader, Abdu I. Alayash, Brandon J. Reeder, Chris E. Cooper, Comparison of the oxidative reactivity of recombinant fetal and adult human hemoglobin: implications for the design of hemoglobin-based oxygen carriers, Biosci. Rep. 38 (2018), BSR20180370.
[8] J. Yudin, M. Verhovsek, How we diagnose and manage altered oxygen affinity hemoglobin variants, Am. J. Hematol. 94 (2019) 597–603.
[9] K. Ratanasopa, M.B. Strader, A.I. Alayash, L. Bulow, Dissection of the radical reactions linked to fetal hemoglobin reveals enhanced pseudoperoxidase activity, Front. Physiol. 6 (2015) 39.
[10] K. Ratanasopa, T. Cedervall, L. Bülow, in: Possibilities of Using Fetal Hemoglobin as a Platform for Producing Hemoglobin-Based Oxygen Carriers (HBOCs), Oxygen Transport to Tissue XXXVII Advances in Experimental Medicine and Biology, Springer, New York, 2016, pp. 445–453.
[11] H. Kirpalani, R.K. Whyte, C. Andersen, E.V. Asztalos, N. Heddle, M.A. Blajchman, A. Peliowski, A. Rios, M. LaCorte, R. Connelly, K. Barrington, R.S. Roberts, The premature infants in need of transfusion (pint) study: a randomized, controlled trial of a restrictive (LOW) versus liberal (HIGH) transfusion threshold for extremely low birth weight infants, J. Pediatr. 149 (2006) 301–307.e3.
[12] Fetus, R.K. Whyte, A.L. Jefferies, C.P. Society, N. Committee, Red blood cell transfusion in newborn infants, Paediatr. Child Health 19 (2014) 213–217.
[13] M. Bianchi, P. Papacci, C.G. Valentini, O. Barbagallo, G. Vento, L. Teofili, Umbilical cord blood as a source for red-blood-cell transfusion in neonatology: a systematic review, Vox Sang. 113 (2018) 713–725.
[14] R.M. Patel, A. Knezevic, N. Shenvi, M. Hinkes, S. Keene, J.D. Roback, K.A. Easley, C.D. Josephson, Association of red blood cell transfusion, anemia, and necrotizing enterocolitis in very low-birth-weight infants, JAMA 315 (2016) 889–897.
[15] X. Zhao, J. Zhou, G. Du, J. Chen, Recent advances in the microbial synthesis of hemoglobin, Trends Biotechnol. 39 (2021) 286–297.
[16] M.J. Weickert, M. Pagratis, S.R. Curry, R. Blackmore, Stabilization of apoglobin by low temperature increases yield of soluble recombinant hemoglobin in *Escherichia coli*, Appl. Environ. Microbiol. 63 (1997) 4313–4320.
[17] M.B. Strader, T. Kassa, F. Meng, F.B. Wood, R.E. Hirsch, J.M. Friedman, A. I. Alayash, Oxidative instability of hemoglobin E (ß26 Glu→Lys) is increased in the presence of free a subunits and reversed by a-hemoglobin stabilizing protein (AHSP): relevance to HbE/ß-thalassemia, Redox Biol. 8 (2016) 363–374.
[18] M.K. Akhtar, P.R. Jones, Cofactor engineering for enhancing the flux of metabolic pathways, Front. Bioeng. Biotechnol. 2 (2014) 30.
[19] P.E. Graves, D.P. Henderson, M.J. Horstman, B.J. Solomon, J.S. Olson, Enhancing stability and expression of recombinant human hemoglobin in *E. coli*: progress in the development of a recombinant HBOC source, BBA-Proteins Proteom. 1784 (2008) 1471–1479.
[20] L. Liu, J.L. Martínez, Z. Liu, D. Petranovic, J. Nielsen, Balanced globin protein expression and heme biosynthesis improve production of human hemoglobin in *Saccharomyces cerevisiae*, Metab. Eng. 21 (2014) 9–16.
[21] W. Kaca, R.I. Roth, J. Levin, Hemoglobin, a newly recognized lipopolysaccharide (LPS)-binding protein that enhances LPS biological activity, J. Biol. Chem. 269 (1994) 25078–25084.
[22] D.L. Currell, J. Levin, The oxidative effect of bacterial lipopolysaccharide on native and cross-linked human hemoglobin as a function of the structure of the lipopolysaccharide, Eur. J. Biochem. 269 (2002) 4635–4640.
[23] S.D. Wright, R.A. Ramos, P.S. Tobias, R.J. Ulevitch, J.C. Mathison, CD14, a receptor for complexes of lipopolysaccharide (LPS) and LPS binding protein, Science 249 (1990) 1431.
[24] M. Tschofen, D. Knopp, E. Hood, E. Stöger, Plant molecular farming: much more than medicines, Annu Rev Anal Chem (Palo Alto, Calif) 9 (2016) 271–294.
[25] R. Tanaka, A. Tanaka, Tetrapyrrole biosynthesis in higher plants, Annu. Rev. Plant Biol. 58 (2007) 321–346.
[26] G. Friso, K.J. van Wijk, Posttranslational protein modifications in plant metabolism, Plant Physiol. 169 (2015) 1469–1487.
[27] M. Sabalza, P. Christou, T. Capell, Recombinant plant-derived pharmaceutical proteins: current technical and economic bottlenecks, Biotechnol. Lett. 36 (2014) 2367–2379.
[28] W. Dieryck, J. Poyart, M. Marden, V. Gruber, P. Bournat, S. Baudino, B. Merot, Human haemoglobin from transgenic tobacco, Nature 386 (1997) 29–30.
[29] S. Schulz, A. Stephan, S. Hahn, L. Bortesi, F. Jarczowski, U. Bettmann, A.-K. Paschke, D. Tusé, C.H. Stahl, A. Giritch, Y. Gleba, Broad and efficient control of major foodborne pathogenic strains of *Escherichia coli* by mixtures of plant-produced colicins, Proc. Natl. Acad. Sci. U. S. A. 112 (2015) E5454–E5460.
[30] D.Z. Silberstein, K. Karuppanan, H.H. Aung, C.-H. Chen, C.E. Cross, K.A. McDonald, An oxidation-resistant, recombinant alpha-1 antitrypsin produced in *Nicotiana benthamiana*, Free Radic. Biol. Med. 120 (2018) 303–310.
[31] S. Torti, R. Schlesier, A. Thümmler, D. Bartels, P. Römer, B. Koch, S. Werner, V. Panwar, K. Kanyuka, N.V. Wirén, J.D.G. Jones, G. Hause, A. Giritch, Y. Gleba, Transient reprogramming of crop plants for agronomic performance, Nat. Plants 7 (2021) 159–171.
[32] M.L.R. Carlsson, S. Kanagarajan, L. Bülow, L.-H. Zhu, Plant based production of myoglobin - a novel source of the muscle heme-protein, Sci. Rep. 10 (2020) 920.
[33] S. Hahn, A. Giritch, D. Bartels, L. Bortesi, Y. Gleba, A novel and fully scalable *Agrobacterium* spray-based process for manufacturing cellulases and other cost-sensitive proteins in plants, Plant Biotechnol. J. 13 (2015) 708–716.
[34] G.P. Lomonossoff, M.-A. D'Aoust, Plant-produced biopharmaceuticals: a case of technical developments driving clinical deployment, Science 353 (2016) 1237–1240.
[35] L. Feng, D.A. Gell, S. Zhou, L. Gu, Y. Kong, J. Li, M. Hu, N. Yan, C. Lee, A.M. Rich, R.S. Armstrong, P.A. Lay, A.J. Gow, M.J. Weiss, J.P. Mackay, Y. Shi, Molecular mechanism of AHSP-mediated stabilization of α-hemoglobin, Cell 119 (2004) 629–640.
[36] K. Ratanasopa, Human Fetal Hemoglobin: Biochemical Characterization and Recombinant Production, Lund University, Sweden, 2015.
[37] M. Kozak, The scanning model for translation - an update, J. Cell Biol. 108 (1989) 229–241.
[38] J.A. Lindbo, TRBO: a high-efficiency tobacco mosaic virus RNA-based overexpression vector, Plant Physiol. 145 (2007) 1232–1240.
[39] K. Kettisen, M.B. Strader, F. Wood, A.I. Alayash, L. Bülow, Site-directed mutagenesis of cysteine residues alters oxidative stability of fetal hemoglobin, Redox Biol. 19 (2018) 218–225.
[40] M. Gram, U. Dolberg Anderson, M.E. Johansson, A. Edström-Hägerwall, I. Larsson, M. Jälmby, S.R. Hansson, B. Åkerström, The human endogenous protection system against cell-free hemoglobin and heme is overwhelmed in preeclampsia and provides potential biomarkers and clinical indicators, PLoS One 10 (2015), e0138111.
[41] E. Antonini, M. Brunori, Hemoglobin and Myoglobin in Their Reactions With Ligands Vol. 21, 1971. North-Holland, Amsterdam.
[42] Z. Chu, Y. Wang, G. You, Q. Wang, N. Ma, B. Li, L. Zhao, H. Zhou, The P50 value detected by the oxygenation-dissociation analyser and blood gas analyser, Artif. Cells Nanomed. Biotechnol. 48 (2020) 867–874.

[43] W. Yan, L. Shen, W. Yu, Y. Wang, Q. Wang, G. You, L. Zhao, H. Zhou, T. Hu, A triply modified human adult hemoglobin with low oxygen affinity, rapid autoxidation and high tetramer stability, Int. J. Biol. Macromol. 159 (2020) 236–242.
[44] B. Li, X. Zhu, M.A. Hossain, C.R. Guy, H. Xu, J. Bungert, B.S. Pace, Fetal hemoglobin induction in sickle erythroid progenitors using a synthetic zinc finger DNA-binding domain, Haematologica 103 (2018), e384.
[45] T. Kassa, S. Jana, F. Meng, A.I. Alayash, Differential heme release from various hemoglobin redox states and the upregulation of cellular heme oxygenase-1, FEBS Open Bio 6 (2016) 876–884.
[46] Q. Wang, R. Zhang, M. Lu, G. You, Y. Wang, G. Chen, C. Zhao, Z. Wang, X. Song, Y. Wu, L. Zhao, H. Zhou, Bioinspired polydopamine-coated hemoglobin as potential oxygen carrier with antioxidant properties, Biomacromolecules 18 (2017) 1333–1341.
[47] T. Yagami, B.T. Ballard, J.C. Padovan, B.T. Chait, A.M. Popowicz, J.M. Manning, N-terminal contributions of the γ-subunit of fetal hemoglobin to its tetramer strength: remote effects at subunit contacts, Protein Sci. 11 (2002) 27–35.
[48] H. Xu, E.J. Bjerneld, M. Käll, L. Börjesson, Spectroscopy of single hemoglobin molecules by surface enhanced raman scattering, Phys. Rev. Lett. 83 (1999) 4357–4360.
[49] M.B. Strader, W.A. Hicks, T. Kassa, E. Singleton, J. Soman, J.S. Olson, M.J. Weiss, T.L. Mollan, M.T. Wilson, A.I. Alayash, Post-translational transformation of methionine to aspartate is catalyzed by heme iron and driven by peroxide: a novel subunit-specific mechanism in hemoglobin, J. Biol. Chem. 289 (2014) 22342–22357.
[50] K. Taguchi, Y. Urata, M. Anraku, T. Maruyama, H. Watanabe, H. Sakai, H. Horinouchi, K. Kobayashi, E. Tsuchida, T. Kai, M. Otagiri, Pharmacokinetic study of enclosed hemoglobin and outer lipid component after the administration of hemoglobin vesicles as an artificial oxygen carrier, Drug Metab. Dispos. 37 (2009) 1456–1463.
[51] A. Dumoulin, L.R. Manning, W.T. Jenkins, R.M. Winslow, J.M. Manning, Exchange of subunit interfaces between recombinant adult and fetal hemoglobins: evidence for a functional inter-relationship among regions of the tetramer, J. Biol. Chem. 272 (1997) 31326–31332.
[52] M.J. Weickert, S.R. Curry, Turnover of recombinant human hemoglobin in *Escherichia coli* occurs rapidly for insoluble and slowly for soluble globin, Arch. Biochem. Biophys. 348 (1997) 337–346.
[53] A.U. Igamberdiev, C. Seregélyes, N. Manac'h, R.D. Hill, NADH-dependent metabolism of nitric oxide in alfalfa root cultures expressing barley hemoglobin, Planta 219 (2004) 95–102.
[54] P. Pratibha, S.K. Singh, R. Srinivasan, S.R. Bhat, Y. Sreenivasulu, Gametophyte development needs mitochondrial coproporphyrinogen III oxidase function, Plant Physiol. 174 (2017) 258–275.
[55] H. Lai, M. Engle, A. Fuchs, T. Keller, S. Johnson, S. Gorlatov, M.S. Diamond, Q. Chen, Monoclonal antibody produced in plants efficiently treats West Nile virus infection in mice, Proc. Natl. Acad. Sci. U. S. A. 107 (2010) 2419–2424.
[56] J.F. Buyel, R.M. Twyman, R. Fischer, Extraction and downstream processing of plant-derived recombinant proteins, Biotechnol. Adv. 33 (2015) 902–913.
[57] H. Fu, P.A. Machado, T.S. Hahm, R.J. Kratochvil, C.I. Wei, Y.M. Lo, Recovery of nicotine-free proteins from tobacco leaves using phosphate buffer system under controlled conditions, Bioresour. Technol. 101 (2010) 2034–2042.
[58] S. Hassan, C.J. Van Dolleweerd, F. Ioakeimidis, E. Keshavarz-Moore, J.K.C. Ma, Considerations for extraction of monoclonal antibodies targeted to different subcellular compartments in transgenic tobacco plants, Plant Biotechnol. J. 6 (2008) 733–748.
[59] J.J. Plomer, J.R. Ryland, M.-A.H. Matthews, D.W. Traylor, E.E. Milne, S.L. Durfee, A.J. Mathews, J.O. Neway, Purification of hemoglobin, in: US Patent 5 851, RHB1 ACQUISITION CORP, US, 1998.
[60] D. Petsch, F.B. Anspach, Endotoxin removal from protein solutions, J. Biotechnol. 76 (2000) 97–119.
[61] K.D. Vandegriff, R.M. Winslow, Hemospan: design principles for a new class of oxygen therapeutic, Artif. Organs 33 (2009) 133–138.
[62] A.I. Alayash, Hemoglobin-based blood substitutes and the treatment of sickle cell disease: more harm than help? Biomolecules 7 (2017) 2.
[63] X. Wu, N.T. Ho, T.-J. Shen, V. Vagni, D.K. Shellington, K. Janesko-Feldman, T.C. S. Tam, M.F. Tam, P.M. Kochanek, C. Ho, V. Simplaceanu, Recombinant octameric hemoglobins as resuscitation fluids in a murine model of traumatic brain injury plus hemorrhagic dhock, in: H.W. Kim, A.G. Greenburg (Eds.), Hemoglobin-Based Oxygen Carriers as Red Cell Substitutes and Oxygen Therapeutics, Springer Berlin Heidelberg, Berlin, Heidelberg, 2013, pp. 249–272.
[64] E. Nagababu, S. Ramasamy, J.M. Rifkind, Y. Jia, A.I. Alayash, Site-specific cross-linking of human and bovine hemoglobins differentially alters oxygen binding and redox side reactions producing rhombic heme and heme degradation, Biochemistry 41 (2002) 7407–7415.
[65] C.E. Cooper, G.G.A. Silkstone, M. Simons, B. Rajagopal, N. Syrett, T. Shaik, S. Gretton, E. Welbourn, L. Bülow, N.L. Eriksson, L. Ronda, A. Mozzarelli, A. Eke, D. Mathe, B.J. Reeder, Engineering tyrosine residues into hemoglobin enhances heme reduction, decreases oxidative stress and increases vascular retention of a hemoglobin based blood substitute, Free Radic. Biol. Med. 134 (2019) 106–118.
[66] N. Griffon, V. Baudbin, W. Dieryck, A. Dumoulin, J. Pagnier, C. Poyart, M. C. Marden, Tetramer-dimer equilibrium of oxyhemoglobin mutants determined from auto-oxidation rates, Protein Sci. 7 (1998) 673–680.
[67] K. Sverrisson, J. Axelsson, A. Rippe, M. Gram, B. Åkerström, S.R. Hansson, B. Rippe, Extracellular fetal hemoglobin induces increases in glomerular permeability: inhibition with a1-microglobulin and tempol, Am. J. Physiol. Renal Physiol. 306 (2013) F442–F448.
[68] R. Hickey, A.F. Palmer, Synthesis of hemoglobin-based oxygen carrier nanoparticles by desolvation precipitation, Langmuir 36 (2020) 14166–14172.